Published in final edited form as:
Adv Mater. 2011 October 18; 23(39): 4509–4515. doi:10.1002/adma.201102371.

Nanogel Star Polymer Architectures: A Nanoparticle Platform for Modular Programmable Macromolecular Self-Assembly, Intercellular Transport, and Dual-Mode Cargo Delivery

Victor Y. Lee,
IBM Almaden Research Center San Jose, CA 95120, USA

Karen Havenstrite,
School of Medicine Stanford University Stanford, CA 94305, USA

Melia Tjio,
Department of Chemical and Materials Engineering San Jose State University San Jose, CA 95192, USA

Melanie McNeil,
Department of Chemical and Materials Engineering San Jose State University San Jose, CA 95192, USA

Helen M. Blau,
School of Medicine Stanford University Stanford, CA 94305, USA

Robert D. Miller*, and
IBM Almaden Research Center San Jose, CA 95120, USA

Joseph Sly*
IBM Almaden Research Center San Jose, CA 95120, USA

There is a growing demand for the simultaneous, site-localized delivery and expression of tandem functionality within the human body. [1–7] The benefits of dual delivery of functional cargos such as two (synergistic) therapeutics, [8,9] a therapeutic and an imaging agent, [4,10] or dual-mode imaging agents [11,12] have all been recently reported. For many medical applications requiring such in vivo expression of exogenous functional materials, the use of polymeric nanoparticle delivery vehicles of increasingly complex design is envisioned. Currently, organic nanoparticle platforms under development for these purposes include liposomes, [13] dendrimers,[14] and micelles. [15] Alternatively, star polymers (unimolecular, globular, polymer architectures) are an increasingly attractive class of organic nanoparticles for biomedical research purposes. [16–18] Although topographically similar to dendrimers (i.e., a high local density of polymeric arms, surface functionality, and interstitial regions), they lack the synthetic and structural limitations of dendrimers [19,20] and the dynamic instability of micelles [21] and liposomes. [22] Nanogel star polymers, i.e., those with polymer "arms" emanating from a cross-linked polymer core, [23,24] in particular, offer a potential for variation in nanoparticle structure and surface functional, i.e., arm density but are among the most synthetically demanding of polymeric nanostructures to develop. [25–29]

*rdmiller@almaden.ibm.com; joesly@us.ibm.com .

Supporting Information Supporting Information is available from the Wiley Online Library or from the author.

The nanogel star polymer, as a unimolecular nanoparticle architecture is, in principle, well-suited for exploring the controlled uptake and in vivo delivery of multiple functional cargos (drugs, genetic materials, imaging agents, etc.). The concept of uploading, protecting, stabilizing, enhancing, or transporting functional materials within the accessible confines of a polymeric enclosure is a powerful one with a range of applications. The ability of dendrimers, for example, to form complexes with many functional materials has remained one of their more enticing features with applications ranging from drug delivery [30] to catalysis. [31] Conceivably, not only should nanogel star-polymer architectures mimic dendrimer characteristics but, because of their substantially larger size (10–100 nm), they should also be able to carry more, larger, or even multiple "cargos". Nanogel star polymers have, however, long suffered from difficulties in reproducibility and control of key structural features such as particle size, arm number (polyvalency), and uniformity, all of which provide an impediment to their general application. To enable the nanogel star polymer platform as a delivery vehicle for multimodal in vivo applications and to add this platform to the growing efforts in nanomedicine research, we report a route to uniform, size and chemically controlled nanogel star polymer architectures that are capable of tunable polyvalent functionality, programmable tandem-modal self-assembly with other functional molecules (represented in this work by porphyrinoid dyes and siRNA), and of cargo transport across cellular membranes of dormant progenitor cells.

Nanogel star polymers can be formed either by an "arm first" process [24] in which living polymer arms are "stitched" together using a cross-linking agent or a "core first" [32] approach where the polymer arms are grown from a preformed macro-initiating gel. We have used a combination of both approaches to make core/shell nanogel star polymer architectures (Scheme 1). In this approach, a preformed nanogel star polymer of hydrophobic composition and controlled size, uniformity, and arm number comprises the cross-linked hydrophobic core and emanating arms. This nanogel star polymer scaffold is then peripherally functionalized with initiating groups for subsequent polymerization to install hydrophilic blocks from the end points of the hydrophobic arm sections. The resulting core/shell structure is subsequently used to study solovophobically driven macromolecular occlusion complex formation as one mode of self-assembly. The second assembly mode uses a plurality of ligating substituents located in the outer hydrophillic block to promote interactions such as organometallic ligation with inorganic nanoparticles, catalytic sites for inorganic nanoshell formation, or electrostatic binding of charged biomolecules.

To first create the hydrophobic inner-shell nanogel star polymer section we used polystyrene as the composition and investigated room-temperature anionic polymerization. Previous studies on polystyrene nanogel star polymer synthesis required the use of very low temperature conditions [24,28,32] or a combination of high temperatures and long reaction times. [33] Recent work has however demonstrated that living anionic linear polymerization of styrene derivatives occurs rapidly at room temperature when nonpolar solvents are used. [34] Here, we initiated with commercially available 3-(*tert*-butyldimethylsilyloxy)-1-propyl lithium, which simultaneously installed a latent, synthetically useful functionality in the form of a protected primary alcohol on the nonliving end of the linear polystyrene chain, providing sites for subsequent peripheral functionalization of the star-polymer structure. *para*-Divinylbenzene (*p*-DVB) was chosen as the cross-linking agent based on the demonstrated efficacy of DVB in previous methodologies. [24,35]

Using this approach, a solution of living linear polystyrene arm **1** was first created at room temperature in 20 minutes on a multigram scale (Scheme 1). Gel permeation chromatography (GPC) analysis of a quenched aliquot of the reaction solution showed **1** to have the targeted molecular weight, M_w = 3.3 kDa (degree of polymerization, DP = 32) and low polydispersity index (M_w/M_n) PDI = 1.03 (Figure 1). Subsequent addition of

regioisomerically pure *p*-DVB[36] (1.1% of the mass of the macroinitiator mass) to the solution of **1** at room temperature resulted in a rapid change in the reaction color, from orange to deep red. After 40 minutes, the reaction was simultaneously quenched and isolated by direct precipitation from (deoxygenated) methanol. GPC analysis of the crude product showed the formation of a monomodal, high-molecular-weight species of low polydisperisty (*PDI* = 1.21) in approximately 80% yield. The only lower molecular weight material present was the residual linear polymer arm **1** (approximately 20% of the crude product). Owing to the high uniformity of **2a**, the crude product could be readily purified by a single preparative solvent fractionation process. The viscous oil thus produced was subsequently re-precipitated into methanol to afford the nanogel star polymer **2a** isolated as a white, amorphous, free-flowing powder in 75% overall yield on (up to) a 50 g scale (Figure 1).

Nanogel star polymer **2a** was soluble in a range of organic solvents in which the component linear arms were also soluble. GPC analysis of **2a** indicated a monomodal distribution of high-molecular-weight material, free of residual linear arms (Figure 1). Inverse gated ^{13}C NMR spectroscopy indicated the highly syndiotactic nature of **2a**, which also had a relatively low glass transition temperature (T_g = 89 °C, determined by differential scanning calorimetry) for such a high-molecular-weight polymer, as is often the case for these type of architectures. Thermal gravimetric analysis showed **2a** was more resistant to thermal degradation than the linear arm **1**. Dynamic light scattering (DLS) of **2a** indicated a M_w = 104 kDa with a *PDI* = 1.12 and a hydrodynamic radius (R_h) = 5.5 nm (tetrahydrofuran (THF)). This corresponds to an average arm number (AAN) of 31 arms per nanogel star polymer **2a**, similar to the end-group number of an AB_2-type fourth-generation dendrimer.

Because the nanogel star polymer **2a** had a similar AAN to that of a typical dendrimer's valency, the capacity to vary both the size and arm number of **2a** was investigated. This was done simply by altering the length of the linear polymer arm and/or the amount of *p*-DVB added in the formation of **2a** (Table 1**).** For example, using a shorter arm length (e.g., M_w = 2.6 kDa) and the same amount of *p*-DVB used to make **2a** produced a smaller nanogel star polymer **2b** with less mass, as expected, but also a lower AAN (M_n = 63 kDa, R_h = 4.2 nm, and AAN = 24). Alternatively, starting with longer linear arms (e.g., M_w = 4.3 kDa) and using different amounts of *p*-DVB, produced uniform nanoparticles but each with different structural parameters. For example, using either 1.8 or 8.6 equivalents of *p*-DVB, resulted in nanogel star polymers **2c** (M_n = 97 kDa, R_h = 5 nm, and AAN = 24) or **2d** (M_n = 544 kDa, R_h = 10 nm, and AAN = 93). In this way, different pairs of nanogel star-polymers samples were created in which their structural parameters approximated cases where the two nanoparticles had: i) the same valency but different sizes, i.e., **2d** and **2e**, both 24 arm particles but with R_h = 5 and 16 nm, respectively; ii) the same size but different valencies, i.e., **2e** and **2f**, both with R_h = 16 nm but with AAN = 24 or 48, respectively; and iii) the default case in which both the size and valency differed but the chemical composition remained the same, i.e., **2d** and **2f**. These results demonstrate an exquisite level of control over the structural parameters of these highly uniform nanoparticles (Figure 2). This high structural uniformity and control in the formation of **2a**, combined with the rapid, scalable, room-temperature synthesis provides one of the most improved and attractive procedures for obtaining polystyrene nanogel star polymers architectures. [33,37–41] In the context of this work, this level of control provided the scaffold versatility required for the continued evolution of the nano particle structure.

The latent peripheral functionality of the nanogel star polymer **2a** was readily activated to produce the primary alcohol functionalized nanogel star polymer **3**. The *tert*-butyldimethylsilyloxy protecting groups from the periphery of star polymer **2a** could be removed using tetrabutylammonium fluoride (TBAF), again at room temperature, without any discernable changes to its structural characteristics (as determined by DLS). The

chemical transformation was monitored by ^{1}H NMR analysis, which showed the quantitative loss of the organosilane signals of **2a** at 0.5 and 0.9 ppm after conversion into the alcohol functionalized nanogel star polymer **3**. The star polymer **3** was then transformed into a nanogel macroinitiator **4** by coupling the alcohol groups of **3** to 2-bromoisobutyrylbromide, again without any observable changes to the structural parameters of **4**. This peripheral functionalization was quantitatively determined by ^{1}H NMR analysis. Along with the appearance of bromoisobutyryl signals at 0.85 ppm, the signal from the CH_2 group alpha to the OH group in **3** shifted downfield from 3.45 to 3.78 ppm in **4** (400 MHz, $CDCl_3$) as expected after esterification.

The nanogel star polymer **4** was then used as a macroinitiator for the formation of water soluble core/shell nanogel star polymers. Linear polymers (< 10 kDa) of *N*,*N*-dimethyl-aminoethyl methacrylate p(DMAEMA) have been recently reported to exhibit low in vitro toxicity. [43] Consequently, p(DMAEMA), a material of increasing biological importance in its own right, [18,42] was used to form the outer shell sections that contained a plurality of pendant ligating amines. The outer shell thickness was also tuned to provide nanoparticles of ≈25 nm, a size predicted to approximate the theoretical optimum for endocytotic uptake into animal cells. [44] Atom transfer radical polymerization (ATRP) [45] was used because it is amenable to many functional monomers, depending on the desired outer shell functionality and nanoparticle properties, and the terminal bromide functionality formed provides a handle for further surface transformations, e.g., attachment of cellular targeting agents. [46] Macroinitiator **4** was effective for polymerizing DMAEMA (Scheme 1) on a gram scale to form the core/shell nanogel star polymer **5** with a hydrophillic, polyamine outer shell of p(DMAEMA). ^{1}H NMR analysis of **5** indicated an average of 19 units of DMAEMA (M_n = 3.0 kDa) were added to each polystyrene arm of **4**. GPC analysis of **5** shows a single species with a monomodal molecular weight distribution higher than that of **4** (Figure 1). DLS measurements of **5** indicated M_n = 274 kDa, *PDI* = 1.22, and R_h = 12 nm (THF). The core/shell nanoparticle **5** is soluble in a range of organic solvents. It is also water soluble, aided by predissolution with a miscible organic solvent, such as acetone, that is later removed under reduced pressure, producing aqueous solutions stable under physiological conditions. In water at 37 °C, **5** is positively charged (zeta-potential ζ = +36 mV), presumably arising from protonation of the pendant amino groups in the outer shell. Atomic force microscopy (AFM) images of silicon wafers dip-coated with aqueous solutions of **5** show discrete, highly uniform, globular nanoparticles of ≈10 nm average radius in the solid state (Figure 1).

As an example of hydrophobically driven macromolecular self-assembly, the capacity of core/shell nanogel star polymer **5** to form aqueous solution of occlusion complexes with large hydrophobic functional macromolecules was demonstrated. Porphyrinoids were selected for this purpose because they are ubiquitous in natural functional systems [47] as well as in many emerging artificial ones. [48] The ability to deliver these large and often hydrophobic, naturally aggregating, strongly absorbing macrocycles in vivo is extremely difficult but in high demand both as fluorescence imaging agents and for emerging photodynamic treatments of tumors and other ailments. [49–51] Two different porphyrinoids were chosen for this study. 5,10,15,20-(3,5-Di-*tert*-butyphenyl) porphyrin **6a** with molar absorbtivities (CH_2Cl_2) of 5.6×10^5 mol^{-1} cm^{-1} at 421 nm and 6.9×10^3 mol^{-1} cm^{-1} at 649 nm (Figure 3) is extremely hydrophobic but is substituted to minimize aggregation and fluorescence quenching even at high concentrations. β-Tetra(*b*-*tert*-butyl)-phthalocyanaine **6b**, also extremely hydrophobic, is an intensely absorbing near-infrared (NIR) dye that is somewhat more prone to concentration-dependent aggregation. The nanogel star polymer **5** was effective in providing instant, stable, aqueous formulations of both **6a** and **6b**. The rapid drop-wise addition of a solution of star-polymer **5** and either **6a** or **6b** in THF to water immediately resulted in a colored aqueous solution with the characteristic hue of the

respective dye material as it appeared in organic solution. Excess (non-occluded) dye and THF were easily removed to produce clear, homogeneous, and uniformly colored aqueous solutions of the occlusion complexes **7a** and **7b**, from the cargos **6a** or **6b**, respectively (Figure 3). The further addition of water to the aqueous solutions of **7a** or **7b** had no visible effect on the homogeneity of the solution, which appeared to be stable indefinitely under ambient conditions.

The absorption and emission spectra of the aqueous occlusion complexes **7a** and **7b** revealed a number of striking features. Importantly, both absorption and emission spectra of **7a** were essentially that of the unbound dye **6a** measured in organic solvent, e.g., THF, with only a slight bathochromic shift in the former (Figure 3). This is indicative of the sterically encumbered porphyrin macrocycle **6a** existing in a largely non-aggregated state within the aqueous occlusion complex **7a** and hence **7a** is strongly fluorescent. The actual location of the cargo within the nanoparticle structure has yet to be fully determined and is the subject of ongoing research. Quantitative UV-vis analysis of this material in THF solution suggests that on average ≈12 dye macromolecules are associated with each polymer complex of **7a**, making these cargo-loaded nanoparticles extremely bright, organic equivalents of inorganic quantum dots. In contrast, the aqueous occlusion complex **7b** is not strongly emissive. The absorption spectrum of **7b** shows significant attenuation and hypsochromic shifting of the phthalocyanine q-bands forming a single broad maximum at 620 nm and a hypsochromic shift of the b-band to 343 nm, in comparison with the spectrum for **6a** in THF (see Supporting Information). The resulting spectra is typical of aggregated phthalocyanines and closely approximates that calculated for a cofacial dimer, [52] with no contributions from monomeric or trimeric species observable in the spectrum. This suggests that the cargo in **7b** is confined within relatively large, defined pockets, formed within the interstitial regions of the nanoparticles interior, which can accommodate only limited degrees of aggregation. The dynamic reversibility of the nanogel star polymer occlusion complexes was demonstrated by injection of the aqueous occlusion complex solution **7b** into THF, which regenerated an absorption spectrum identical to that of the free dye **6b** in this solvent, indicating the release of the dye upon the removal of the solvophobic constraint. Preliminary experiments confirm that in aqueous solution the loaded nanoparticles do not appear to exchange cargos, offering the possibility of therapeutic applications involving delivery of multiple, separated, and even potentially mutually reactive, cargos using this nanoparticle platform.

The capability of the nanogel star polymer **5** to transport cargo across cellular membranes was demonstrated next. Cationic polymers are often known to be internalized by cells through non-specific endocytosis [53] and nanogel star poly mer **5** is, by design, potentially a suitable carrier for this purpose. Consequently, primary murine myoblasts were incubated in an aqueous solution of Dulbecco's modified Eagle's medium (DMEM) media containing 10% fetal bovine serum and **7a** (0.5 μg mL^{-1}) overnight and the results were imaged using high-resolution confocal microscopy. The images obtained of the myoblasts (Figure 4) show strong fluorescence intensity localized throughout the cytosol, in pockets likely to be endosomal vesicles, indicating that **7a** had successfully crossed the cell membrane into the intracellular space, transporting its fluorescent cargo along with it. In order to test the viability of the cells containing the internalized nanoparticles and to demonstrate a proof-of-principle imaging application, the cells loaded with **7a** were then further cultured in particle-free media for several days while monitoring the fluorescence intensity of the population using a flow cytometer. After 24 hours the fluorescence intensity of the population was reduced by a factor of ≈3.5. When cells divide, each daughter cell receives half of the initial cytosol and thus after one division we should observe that the fluorescence intensity is reduced by a factor 2. The reduction observed over 24 hours is consistent with the cell division rate of myoblasts of once every 12–18 hours. After 72 hours, the average fluorescence intensity was again further reduced, this time by a factor of ≈8, which is again

consistent with the myoblast division rate. Myoblasts loaded with **7a** were both viable and capable of differentiating into myotubes, indicating that the nanoparticles did not affect the functional viability of the cells over this time (Figure 4).

Finally, the ability of the star polymer occlusion complex **7a** to form electrostatic complexes with double-stranded small interfering RNA (siRNA) was studied to validate the concept of tandem mode self-assembly. The recent demonstrated ability of siRNA to knock down a wide variety of genes has generated a surge of interest in siRNA use for biological and biomedical research. [54–56] The ability to introduce negatively charged genetic materials directly across cellular membranes is, however, problematic and most often enhanced through the use of synthetic vectors for transfection purposes. [57] For these reasons we explored the potential of binding negatively charged siRNA to the cationic exterior outer shell of the nanogel star polymer occlusion complex **7a** using electrostatic complexation. The occlusion complex **7a** was incubated with a random 21 nucleotide siRNA sequence **8** for 30 minutes at room temperature to produce the dual-functional nanogel star polymer **9** (Scheme 1). Electrophoretic analysis of the solutions formed from incubating **7a** with siRNA **8** in ratios varying from 1:1 to 1:50 (particles:siRNA) indicate that between 5 and 10 individual stands of the siRNA spontaneously bind to **7a** (Figure 3). The capacity to complex both dyes and genetic material to a single delivery vehicle provides a luminescent tracking route for both single- and double-stranded genetic material delivery, removing the need for covalent attachment of the dye to the genetic material, a capability that will, in principle, greatly aid in the further development of siRNA for therapeutic purposes. The performance of complex **9** as a gene carrier, in terms of properties such as complex stability, protection of the genetic material from enzymatic degradation, and transfection efficiency are currently under investigation.

In summary, we have developed a versatile and convenient approach to produce uniform, structurally versatile, water-soluble, unimolecular polymeric nanoparticles capable of up-loading various cargos through tandem macromolecular self-assembly. Key to this approach is the development of a rapid, scalable, room-temperature anionic polymerization for the arm first production of polystyrene-based nanogel star polymers that can be used to tune key nanoparticle parameters such as size, polyvalency, and peripheral functionality. These functionalized nanoparticles can then, in turn, be used as macroinitiators in a core first fashion to produce core/shell nanogel star polymer nanoparticles, again with good control over their uniformity and innate peripheral functionality. The core/shell nanogel star polymers were successfully preprogrammed to spontaneously upload different types of complex functional macromolecules such as porphyrinoids and siRNA via tandem self-assembly and transport cargo into the interior of primary murine myoblast cells while maintaining cellular viability. These proof-of-principle results provide a demonstration of the potential use of such nanogel star polymer nanoparticles as a highly uniform, tunable, and modular platform for the formation of dual-mode functional polymeric nanoparticles systems for future targeted applications in the areas of synergistic therapeutic delivery, imaged therapeutic delivery, and dual-mode bio-imaging agents. They now also set the stage for a wide variety of alternate chemical compositions, e.g., biodegradable polymers, to be further incorporated into this nanogel star polymer platform for these purposes.

Supplementary Material

Refer to Web version on PubMed Central for supplementary material.

Acknowledgments

The authors thank Philip J. Brock for scale-up assistance; Teddie Magibitang, Dolores Miller, and Jane E. Frommer for technical assistance with GPC and light scattering analysis, NMR experiments, and AFM analysis, respectively; Jennifer Brady for technical assistance with the siRNA binding study and the kind donation of the siRNA. They additionally thank the NIH (training Grant 2 T32 HD007249 to K.H.), the Baxter Foundation, NIH (AG02961 and HL096113), CIRM (Rt1-01001-1) (for H.B.), and the NSF-funded Centre of Polymeric Interfaces and Macrocyclic Assemblies (CPIMA) under award (DMR-9400354) (for R.D.M and J.S.) for financial support of this work.

References

[1]. Lim E-K, Yang Y-MHJ, Lee K, Suh J-S, Haam S. Adv. Mater. 2011; 23:2426.

[2]. Janib SM, Moses AS, Mackay JA. Adv. Drug Delivery Rev. 2010; 62:1052.

[3]. Hao R, Xing R, Xu Z, Hou Y, Gao S, Sun S. Adv. Mater. 2010; 22:2729. [PubMed: 20473985]

[4]. Horcajada P, Chalati T, Serre C, Gillet B, Sebrie C, Baati T, Eubank JF, Heurtaux D, Clayette P, Kreuz C, Chang J-S, Hwang Y, Marsaud V, Bories P-N, Cynober L, Gil S, Férey G, Couvreur P, Grefruxandra R. Nat. Mater. 2009; 9:172. [PubMed: 20010827]

[5]. Na HB, Song IC, Hyeon T. Adv. Mater. 2009; 21:2133.

[6]. Peer D, Karp JM, Hong S, Farokhzad OC, Margalit R, Langer R. Nat. Nanotechnol. 2007; 2:751. [PubMed: 18654426]

[7]. Service RF. Science. 2005; 310:1132. [PubMed: 16293748]

[8]. Wang Y, Gao S, Ye W-H, Yoon HS, Yang Y-Y. Nat. Mater. 2006; 5:791. [PubMed: 16998471]

[9]. Nishiyama N, Iriyama A, Jang W-D, Miyata K, Itaka K, Inoue Y, Takahashi H, Yanagi Y, Tamaki Y, Koyama H, Kataoka K. Nat. Mater. 2005; 4:934. [PubMed: 16299510]

[10]. Park J-H, von Maltzahn G, Ruoslahti E, Bhatia SN, Sailor MJ. Angew. Chem. Int. Ed. 2008; 47:7284.

[11]. Medarova Z, Pham W, Kim Y, Dai G, Moore A. Int. J. Cancer. 2006; 118:2796. [PubMed: 16385568]

[12]. Glaus C, Rossin R, Welch MJ, Bao G. Bioconjugate Chem. 2010; 21:715.

[13]. Wang T, D'Souza GGM, Bedi D, Fagbohun OA, Potturi LP, Papahadjopoulos-Sternberg B, Petrenko VA, Torchilin VP. Nanomedicine. 2010; 5:563. [PubMed: 20528452]

[14]. Kojima C, Regino C, Umeda Y, Kobayashi H, Kono K. Int. J. Pharm. 2010; 383:293. [PubMed: 19761822]

[15]. Gref R, Minamitake Y, Peracchia MT, Trubetskoy V, Torchilin V, Langer R. Science. 1994; 263:1600. [PubMed: 8128245]

[16]. Bencherif SA, Gao H, Srinivasan A, Siegwart DJ, Hollinger JO, Washburn NR, Matyjaszewski K. Biomacromolecules. 2009; 10:1795. [PubMed: 19518096]

[17]. Fukukawa K-I, Rossin R, Hagooly A, Pressly ED, Hunt JN, Messmore BW, Wooley KL, Welch MJ, Hawker CJ. Biomacromolecules. 2008; 9:1329. [PubMed: 18338840]

[18]. Georgiou TK, Vamvakaki M, Phylactou LA, Patrickios CS. Biomacromolecules. 2005; 6:2990. [PubMed: 16283718]

[19]. Astruc D, Boisselier E, Ornelas C. Chem. Rev. 2010; 110:1857. [PubMed: 20356105]

[20]. Tomalia DA. Prog. Polym. Sci. 2005; 30:294.

[21]. Bae YH, Yin H. J. Controlled Release. 2008; 131:2.

[22]. Samad A, Sultana Y, Aqil M. Curr. Drug Delivery. 2007; 4:297.

[23]. Blencowe A, Tan JF, Goh TK, Qiao GG. Polymer. 2009; 50:5.

[24]. Zilliox JG, Rempp P, Parrod J. J. Polym. Sci. Polym. Symp. 1968; 22:145.

[25]. Shibata T, Kanaoka S, Aoshima S. J. Am. Chem. Soc. 2006; 128:7497. [PubMed: 16756304]

[26]. Gao H, Ohno S, Matyjaszewski K. J. Am. Chem. Soc. 2006; 128:15111. [PubMed: 17117861]

[27]. Terashima T, Kamigaito M, Baek K-Y, Ando T, Sawamoto M. J. Am. Chem. Soc. 2003; 125:5288. [PubMed: 12720436]

[28]. Bosman AW, Vestberg R, Heumann A, Fréchet JMJ, Hawker C. J. Am. Chem. Soc. 2003; 125:715. [PubMed: 12526671]

[29]. Guan Z, Cotts PM, McCord EF, McLain SJ. Science. 1999; 283:2059. [PubMed: 10092223]

[30]. Boas U, Heegaard PMH. Chem. Soc. Rev. 2004; 33:43. [PubMed: 14737508]

[31]. Reek JNH, Arevalo S, Heerbeek RV, Kamer PCJ, Van Leeuwen PWNM. Adv. Catal. 2006; 49:71.

[32]. Eschwey H, Hallensleben ML, Burchard W. Makromol. Chem. 1973; 173:235.

[33]. Xia J, Zhang X, Matyjaszewski K. Macromolecules. 1999; 32:4482.

[34]. Ito H, Knebelkamp A, Lundmark SB, Nguyen CV, Hinsberg WD. J. Polym. Sci., Part A: Polym. Chem. 2000; 38:2415.

[35]. Eschwey H, Burchard W. Polymer. 1975; 16:180.

[36]. Examinations of regioisomerically pure *meta*-DVB as a cross-linking agent or enhancing the presence of the *para* isomer in the commercial grade material by simple distillation resulted in only a marginally better degree of structure control. It was found that the only isomerically pure *para* isomer yielded the best results in terms of product uniformity and yield.

[37]. Zilliox JG, Rempp P. C. R. Chim. 1966; 262:726.

[38]. Rempp P, Franta E. Pure Appl. Chem. 1972; 30:229.

[39]. Lutz PL, Rempp P. Macromol. Chem. 1988; 189:1051.

[40]. Bosman AW, Heumann A, Klaerner G, Benoit D, Frechet JMJ, Hawker CJ. J. Am. Chem. Soc. 2001; 123:6461. [PubMed: 11427091]

[41]. Chi Y, Scroggins ST, Frechet JMJ. J. Am. Chem. Soc. 2008; 130:6322. [PubMed: 18433122]

[42]. Rawlinson L-AB, Ryan SM, Mantovani G, Syrett JA, Haddleton DM, Brayden DJ. Biomacromolecules. 2010; 11:443. [PubMed: 20025269]

[43]. Cai J, Yue Y, Rui D, Zhang Y, Liu S, Wu C. Macromolecules. 2011; 44

[44]. Gao H, Shi W, Freund LB. Proc. Natl. Acad. Sci. USA. 2005; 102:9469. [PubMed: 15972807]

[45]. Tsarevsky NV, Matyjaszewski K. Chem. Rev. 2007; 107:2270. [PubMed: 17530906]

[46]. Maltzahn, G. v.; Ren, Y.; Park, J-H.; Min, D-H.; Kotamraju, VR.; Jayakumar, J.; Fogal, V.; Sailor, MJ.; Ruoslahti, E.; Bhatia, SN. Bioconjugate Chem. 2008; 19:1570.

[47]. Kadish, K. The Porphyrin Handbook. Kadish, K.; Smith, K.; Guilard, R., editors. Academic Press; San Diego: 2003.

[48]. Drain CM, Goldberg I, Sylvain I, Falber A. Top. Curr. Chem. 2005; 245:55.

[49]. Brown SB, Brown EA, Walker I. Lancet Oncology. 2004; 5:497. [PubMed: 15288239]

[50]. Szaciowski K, Macyk W, Drzewiecka-Matuszek A, Brindell M, Stochel G. Chem. Rev. 2005; 105:2647. [PubMed: 15941225]

[51]. Pushpan SK, Venkatraman S, Anand VG, Sankar J, Parmeswaran D, Ganesan S, Chandrashekar TK. Curr. Med. Chem.-Anti-Cancer Agents. 2002; 2:187.

[52]. George RD, Snow AW, Shirk JS, Barger WR. J. Porphyrins Phthalocyanines. 1998; 2:1.

[53]. Verma A, Stellacci F. Small. 2010; 6:12. [PubMed: 19844908]

[54]. Jurreck J. Ang. Chem. Int. Ed. 2010; 49:6258.

[55]. Guo OPC, Snead NM, Trebley J, Hoeprich S, Guo S, Shu Y. Adv. Drug Delivery Rev. 2010; 62:650.

[56]. Cruckhorn S. Nat. Rev. Drug Discovery. 2010; 9:359.

[57]. Ruthardt NB, Brauchle C. Top. Curr. Chem. 2010; 296:283. [PubMed: 21504106]

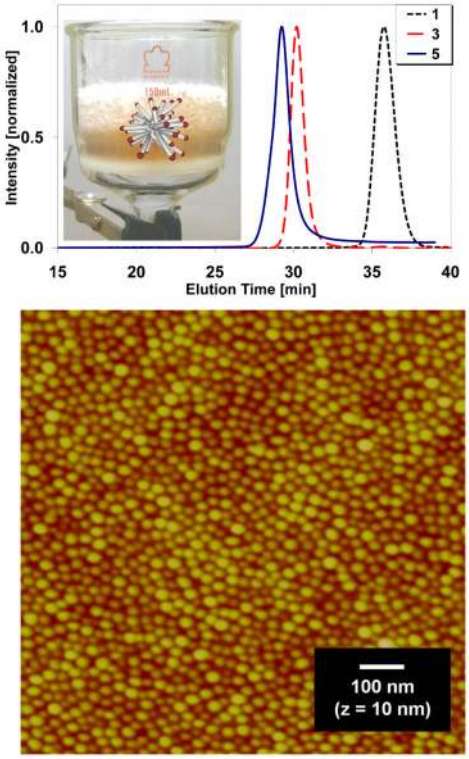

Figure 1.

Top: GPC traces of the linear arm **1**, the hydrophobic core nanogel star polymer **3**, and the core/shell nanogel star polymer **5** showing their high structural uniformity and (inset) photo graph of the result from a single large-scale synthesis of **3**. Bottom: AFM image of **5** deposited from aqueous solution that shows **5** to be discrete uniform globular nanoparticles.

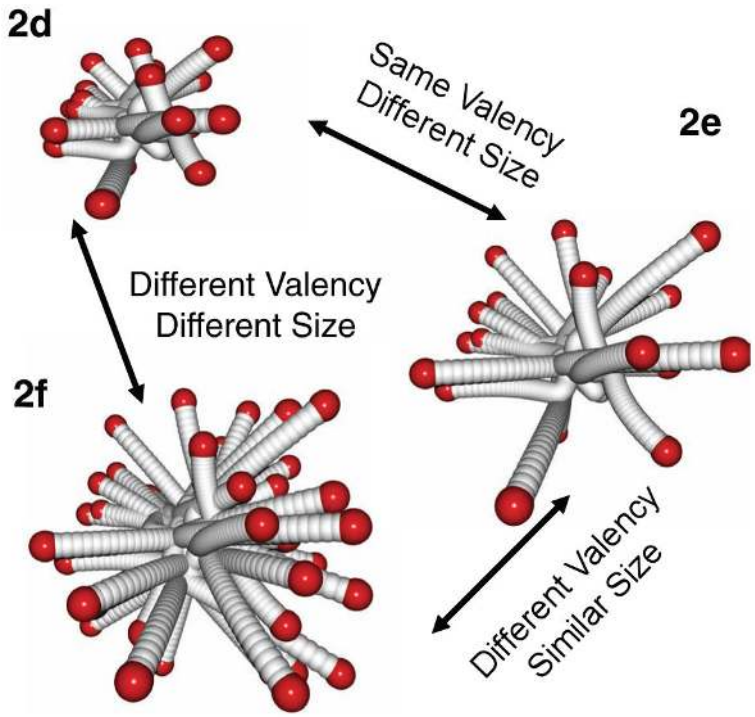

Figure 2.
Cartoon representation of the structural versatility, in terms of controlled nanoparticle size and polyvalency, demonstrated by the formation of **2d–f**.

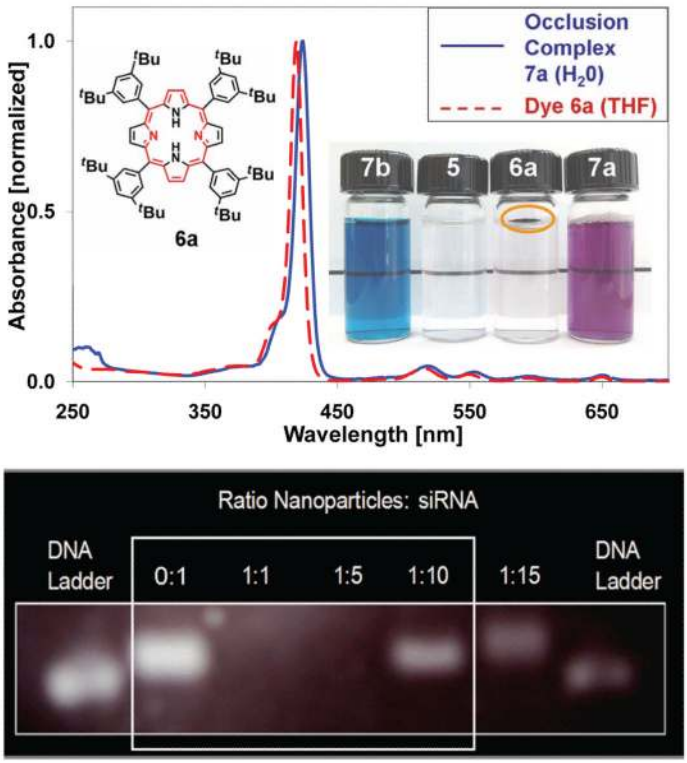

Figure 3.

Spectroscopic analyses of the modular, tandem self-assembly processes used to install dual functionally into the nanogel star polymer delivery platform. Top: Absorption spectra of the occlusion complex **7a** formed from **5** and porphyrin **6a** and a photograph (inset) of the aqueous formulations of **5, 6a** (suspension), and **7a,b**. Bottom: Electrophoretic analysis of the siRNA complexes with **7a** showing the binding of between 5–10 strands of siRNA per dual-functionalized nanoparticle **9**.

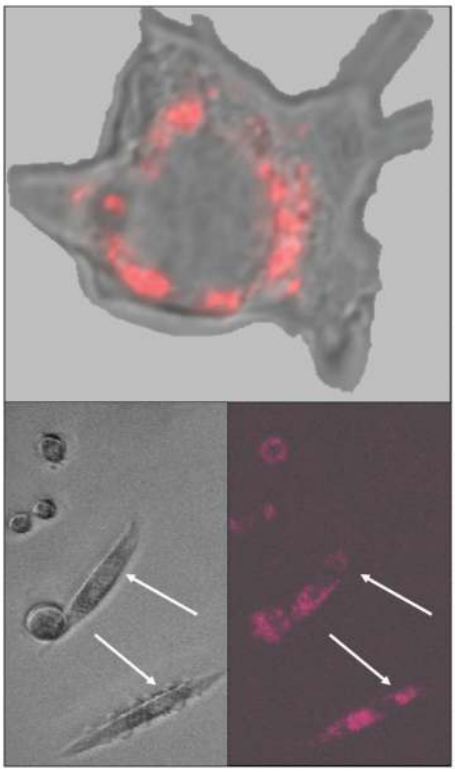

Figure 4.
Top: High-resolution confocal fluorescence microscopy image of a murine muscle myoblast cell after incubation with **7a** showing that the internalized fluorescent nanoparticles have crossed the cellular membrane and are located throughout the cytoplasm of the cell. Bottom: Transmission light microscopy image (right) and confocal fluorescence microscopy image (left) of murine muscle myoblast cells differentiating into myotubes (highlighted by arrows), indicating functional viability of the cells post internalization of **7a**.

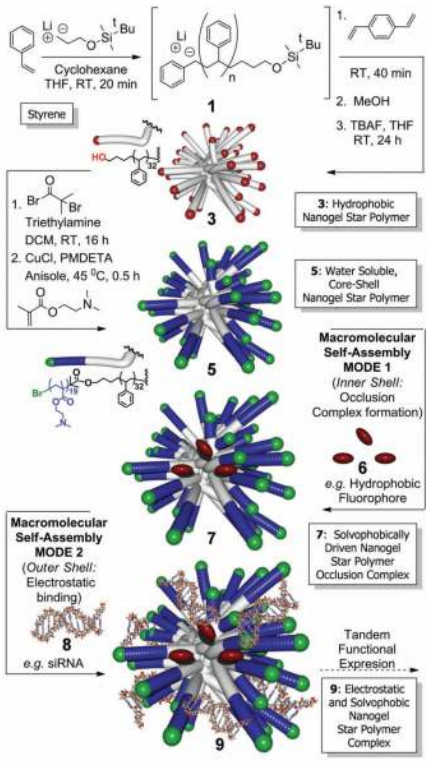

Scheme 1.

Conditions used in the rapid, room-temperature, arm first synthesis of nanogel star polymer **3**, its core first use to create water-soluble core/shell (hydrophobic-hydrophillic) nanogel star polymer **5**, and its subsequent use as a modular preprogrammed tandem-mode macromolecular self-assembly platform **7** and **9** to provide simultaneous expression of functionality (e.g., vehicle for fluorescent delivery of genetic materials shown).

Table 1

The effect of varying arm size and cross-linking reagent (*p*-DVB) amount on the resulting structural parameters of the nanogel star polymers **2a–f**, highlighting the ability to produce highly uniform nanoparticles of controlled size and polyvalency.

			Nanogel Star Size (DLS, THF)			
Entry	**Arm Size: GPC M_n [kg mol^{-1}]**	***p*-DVB [wt%]**	**M_w [kg mol^{-1}]**	***PDI***	**AAN**	**R_h [nm]**
2a	3.3	1.1	104	1.16	31	5.5
2b	2.6	1.0	63	1.19	24	4.2
2c	4.3	8.6	544	1.21	93	10.1
2d	4.3	1.8	97	1.14	*24*	*5.3*
2e	30.6	21.6	725	1.17	*24*	*15.8*
2f	20.2	17.4	935	1.19	*47*	*16.3*

Adv Mater. Author manuscript; available in PMC 2012 October 18.